Molecular Microbiology (2001) **42**(5), 1163–1177

Systematic mutational analysis of the amino-terminal domain of the *Listeria monocytogenes* ActA protein reveals novel functions in actin-based motility

Peter Lauer,[1] Julie A. Theriot,[2] Justin Skoble,[1] Matthew D. Welch[1] and Daniel A. Portnoy[1,3]*
[1]*Department of Molecular and Cell Biology, University of California, Berkeley, CA 94720-3202, USA.*
[2]*Department of Biochemistry, Stanford University School of Medicine, Stanford, CA 94305-5307, USA.*
[3]*School of Public Health, University of California, Berkeley, CA 94720-3202, USA.*

Summary

The *Listeria monocytogenes* ActA protein acts as a scaffold to assemble and activate host cell actin cytoskeletal factors at the bacterial surface, resulting in directional actin polymerization and propulsion of the bacterium through the cytoplasm. We have constructed 20 clustered charged-to-alanine mutations in the NH_2-terminal domain of ActA and replaced the endogenous *actA* gene with these molecular variants. These 20 clones were evaluated in several biological assays for phenotypes associated with particular amino acid changes. Additionally, each protein variant was purified and tested for stimulation of the Arp2/3 complex, and a subset was tested for actin monomer binding. These specific mutations refined the two regions involved in Arp2/3 activation and suggest that the actin-binding sequence of ActA spans 40 amino acids. We also identified a 'motility rate and cloud-to-tail transition' region in which nine contiguous mutations spanning amino acids 165–260 caused motility rate defects and changed the ratio of intracellular bacteria associated with actin clouds and comet tails without affecting Arp2/3 activation. Several unusual motility phenotypes were associated with amino acid changes in this region, including altered paths through the cytoplasm, discontinuous actin tails in host cells and the tendency to 'skid' or dramatically change direction while moving. These unusual phenotypes illustrate the complexity of ActA functions that control the actin-based motility of *L. monocytogenes*.

Accepted 15 August, 2001. *For correspondence. E-mail portnoy@uclink4.berkeley.edu; Tel. (+1) 510 643 3925; Fax (+1) 510 643 5035.

Introduction

Listeria monocytogenes is a Gram-positive facultative intracellular pathogen of many animal species including humans (Farber and Peterkin, 1991). Subsequent to internalization by mammalian cells, *L. monocytogenes* escapes from a vacuole, grows rapidly in the host cytosol and then becomes surrounded by a cloud of actin filaments (reviewed by Cossart and Lecuit, 1998). After a few generations, the actin cloud rearranges into an actin tail, and actin polymerization in this tail propels the bacteria through the cytosol and into neighbouring cells (Tilney and Portnoy, 1989; Mounier *et al*., 1990). Remarkably, a single bacterial protein, ActA, is responsible for actin nucleation and actin-based motility (Domann *et al*., 1992; Kocks *et al*., 1992; 1995; Brundage *et al*., 1993; Pistor *et al*., 1994; Smith *et al*., 1995; Cameron *et al*., 1999). This actin-based motility allows the bacterium to spread from cell to cell without leaving the intracellular environment and avoiding the host immune response.

ActA is a 639-amino-acid membrane protein that is synthesized with a conventional cleavable signal sequence (Domann *et al*., 1992) and a carboxy-terminal transmembrane domain that anchors ActA to the bacterial surface (Kocks *et al*., 1992; Smith *et al*., 1995). ActA has two domains that function in actin-based motility: the NH_2-terminal domain (amino acids 31–263) and the central repeat domain (amino acids 264–390). Actin polymerization is initiated by the interaction of the NH_2-terminal domain of ActA with the host Arp2/3 complex (Welch *et al*., 1998; Skoble *et al*., 2000). The Arp2/3 complex is an evolutionarily conserved, seven polypeptide complex that contains two actin-related proteins and is the host actin nucleation factor (reviewed by Machesky and Gould, 1999) required for bacterial actin-based motility (May *et al*., 1999; Yarar *et al*., 1999). ActA directly and dramatically stimulates the potential of the Arp2/3 complex to nucleate actin polymerization (Welch *et al*., 1998). The first 136 amino acids of the NH_2-terminal domain contain three regions that contribute to Arp2/3-mediated actin nucleation: a stretch of acidic residues ('A' region) and a cofilin homology sequence ('C' region), both of which stimulate the Arp2/3 complex directly, and an actin monomer-binding region ('AB' region) (Skoble *et al*., 2000; Zalevsky *et al*., 2001). Also, within the NH_2-terminal

domain but downstream of the nucleation region is a stretch of residues reported to interact with acidic phospholipids (Cicchetti *et al*., 1999; Steffen *et al*., 2000). The central domain of ActA contains four proline-rich repeats that bind members of the host Enabled/vasodilator-stimulated phosphoprotein (Ena/VASP) family of proteins, which stimulates the movement rate as well as the percentage of moving bacteria (Chakraborty *et al*., 1995; Lasa *et al*., 1995; Smith *et al*., 1996).

Determining the precise mechanism(s) by which ActA functions in a wide variety of different animal species and cell types is of fundamental importance not only to our understanding of listerial pathogenesis, but also to host actin dynamics. *L. monocytogenes* can enter and undergo actin-based motility in virtually all adherent mammalian cells. The movement of *L. monocytogenes* in these cells and between cells is very efficient and reproducible, although movement rates vary more than 10-fold between different cell types and are significantly slower in cell extracts (Dabiri *et al*., 1990; Theriot *et al*., 1994; Smith *et al*., 1996). *L. monocytogenes* has apparently managed to tap into an essential and highly conserved eukaryotic mechanism of actin-based motility. Although aspects of the process can be reproduced in cellular extracts or in biochemical assays (Theriot *et al*., 1994; Welch *et al*., 1998; Loisel *et al*., 1999), the entire process of actin-based motility and cell-to-cell spread can only be studied in live cells. Furthermore, the system is so highly tuned that any alteration in ActA expression level or stability compromises ActA function (Kocks *et al*., 1992; Smith *et al*., 1996; Moors *et al*., 1999a; Pistor *et al*., 2000). To date, there have been many studies to dissect ActA function, but these have been limited by ectopic expression of ActA as well as large deletions or truncations of ActA that may affect domain organization and protein folding (Pistor *et al*., 1994; Friederich *et al*., 1995; Kocks *et al*., 1995; Lasa *et al*., 1995; 1997; Smith *et al*., 1995; 1996; Mourrain *et al*., 1997; Cicchetti *et al*., 1999; Skoble *et al*., 2000). Accordingly, in this study, we have used clustered charged-to-alanine scanning mutagenesis, a method that does not normally alter domain conformation or affect protein folding (Bass *et al*., 1991; Gibbs and Zoller, 1991), and allelic exchange to generate 20 new chromosomal alleles of ActA. Extensive analysis of the mutants has refined the regions of ActA that interact with the Arp2/3 complex and revealed a number of unexpected phenotypes that are Arp2/3 independent.

Results

Design, construction and expression of actA *alleles*

We used a modified 'clustered charged-to-alanine scanning mutagenesis' strategy (Wertman *et al*., 1992), in which the highly charged amino-terminal domain of ActA was arbitrarily divided into 20 sequence blocks (Fig. 1). The 20 new alleles of *actA* were made using site-directed mutagenesis and introduced to the *L. monocytogenes* chromosome by allelic exchange for the expression of each ActA variant using the endogenous transcriptional control elements. The targeted residues and the new restriction site used to identify each *actA* allele are shown in Fig. 1 and Table 1. Each allele was also cloned into an expression vector that replaced the transmembrane sequence with an expressed 6-His tag for purification and *in vitro* biochemical evaluation. In the 10403S (wild-type) background, all the mutant proteins were synthesized and expressed on the bacterial surface in broth

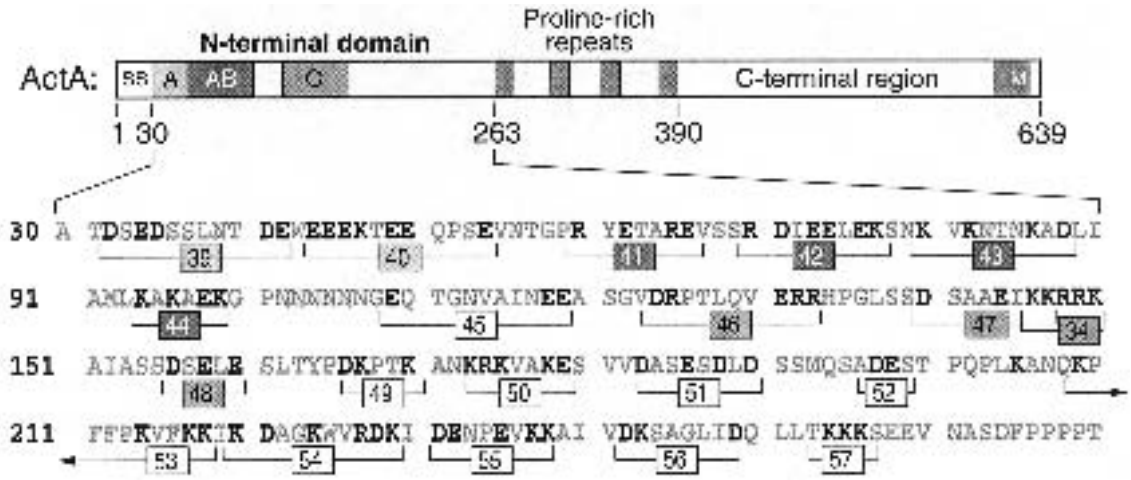

Fig. 1. Amino acids targeted by clustered charged-to-alanine scanning mutagenesis in the NH_2-terminal domain of the ActA protein. Schematic representation of the ActA protein is shown at the top. Primary sequence from amino acids 30–270 is shown at the bottom. Charged amino acids (shown in black and bracketed by mutant number) were divided arbitrarily into blocks and changed *en masse* to alanine (see *Experimental procedures*). Shaded mutant numbers correspond to 'A', 'AB' and 'C' regions of the same colour.

culture at similar levels to wild type (Fig. 2A). Several of the charge alterations had a noticeable effect on the mobility of the ActA protein variants on SDS–PAGE (see mutants 45 and 51, Fig. 2A). Additionally, all secreted variants except mutant 56 were secreted into supernatants at similar levels in the *L. monocytogenes* SLCC-5764 strain background, an *L. monocytogenes* strain that overexpresses the major virulence factors including ActA (Fig. 2B).

To determine whether any of the mutations changed the intracellular expression or stability of the protein variants, we metabolically labelled tissue culture cells infected with each mutant. ActA expression is upregulated in host cells and is one of the most abundant secreted *L. monocytogenes* proteins expressed during intracytoplasmic growth (Brundage *et al*., 1993; Moors *et al*., 1999b). ActA appears as multiple closely migrating bands on SDS–PAGE, a 97 kDa form that co-migrates with *in vitro* expressed ActA plus two additional phosphorylated bands (Brundage *et al*., 1993). The stability of ActA can be determined by a pulse–chase (Moors *et al*., 1999a). All but two of the mutants made a protein that was as stable as wild-type ActA (Fig. 2C; data not shown). The two exceptions were mutants 39 and 56. The stability of mutant 39 ActA was reduced by ≈30% compared with wild type, whereas ActA from mutant 56 was nearly impossible to detect in pulse–chase experiments. Visual inspection of infected J774 cells showed that this mutant was cytotoxic to the host cells, i.e. there were few intact host cells remaining after 4 h of infection, the time point at which proteins are harvested and visualized in the experiment (data not shown). This is in direct contrast to wild type, which causes very little damage to the host cell. These data suggest that there is a secretion defect associated with the mutant 56 protein variant.

In vivo *phenotypes and biochemical assays*

After confirming that each *actA* allele was expressed normally, we used several large-scale quantitative assays to evaluate the effect of each mutation on ActA's function. The quantitative data from these assays – intracellular association with actin, intracellular motility rates, ability of each mutant to spread from cell to cell and the ability of each protein variant to stimulate Arp2/3-mediated actin nucleation – are presented in Fig. 3.

Mutations spanning amino acids 165–260 altered the number of bacteria associated with actin clouds and comet tails and resulted in intracellular motility rate changes

We first assessed the ability of each *actA* mutant to recruit actin to the bacterial surface in infected PtK2 cells by staining for co-localization of F-actin and bacteria. When wild-type *L. monocytogenes* first enters the cytoplasm of the host cell, ActA recruits an actin 'cloud' uniformly around the bacterial surface. This cloud later rearranges to a polar 'comet tail', which provides the propulsive force for bacterial motility. Quantification of the transition from actin clouds to comet tails is an instantaneous and quantitative assessment of which bacteria are moving at any one time. At 4 h after infection, wild-type *L. monocytogenes* was associated with more comet tails than actin clouds (62% and 35% respectively; Fig. 3B). Most of the mutants spanning the Arp2/3 nucleation and actin-binding regions (amino acids 30–165) had a small decrease in the percentage of bacteria associated with comet tails and a small increase in the percentage associated with actin clouds. Exceptions to this trend were those bacterial strains that had an overall decrease in the number of bacteria associated with any actin, notably the contiguous mutants 34 and 48 (in the 'C' region) that combined to have the most severe set of defects in all the assays used to evaluate the mutant panel. Strikingly, all the mutants in the region spanning amino acids 165–260 had an inverted ratio of clouds to tails (Fig. 3B). A strain harbouring an internal deletion of 60 amino acids (Δ202–263, strain DP-L3982; Skoble *et al*., 2000) also had this inverted ratio, suggesting that this region was critical for normal motility inside cells.

We then evaluated the ability of each mutant to undergo actin-based motility using time-lapse video microscopy of infected PtK2 cells. At 4 h after infection, wild-type *L. monocytogenes* moved at an average rate of $6.8 \pm 4.6\ \mu m\ min^{-1}$ (± SD). Movement rates of the mutant panel fell into four categories (Fig. 3C). The first, including mutants 40–47 and 55, was statistically indistinguishable from wild type. The second class moved at an intermediate rate of one-third to three-quarters of the wild-type rate. Mutants 39, 48–52, 54 and 56 fall into this category. Mutant 56 had to be tracked at 6 h after infection in order to observe any moving bacteria, presumably to allow time for the secretion of enough ActA to the bacterial surface to induce motility. The third class of mutant, represented only by mutant 34, did not move in PtK2 cells. The fourth class of mutant moved statistically faster than wild type. The mean rates of mutants 53 and 57 were 117% and 115% of the wild-type rate respectively. Indeed, mutant 57 was tracked at speeds up to $33\ \mu m\ min^{-1}$, or $11\ \mu m\ min^{-1}$ faster than the fastest wild-type bacterium.

We also infected MDCK cells with the mutant panel and found that mutants 39 and 34 had cell type-dependent motility rate phenotypes. As MDCK cells are columnar, have many focal planes and are not as phase transparent as PtK2 cells, it was not possible to gather data on as many individual bacteria as in PtK2 cells. Although mutant 39 (in the 'A' region) moved at half the wild-type rate in PtK2 cells, in MDCK cells, the movement rate was indistinguishable from wild type (wild-type rate: 14.1 ±

Table 1. Residues targeted and oligonucleotides used for *actA* mutagenesis.

Mutant	Strain	AAs changed[a]	Oligonucleotide sequence[b]	RE change
39	DP-L4101	32-DSEDSSLNTDE	TTTGCAGCGACAGCTAGCGCAGCTTCCAGTCTAAACACAGCTGCATGGGAAGAA	*Nhe*I
40	DP-L4102	44-EEEKTEEQPSE	ACAGATGAATGGGCAGCGGCTGCAACAGCTGCGCAGCCAAGCGCGGTAAATACG	*Pvu*II, *Fsp*I
41	DP-L4103	60-RYETARE	AATACGGGACCAGCATACGCAACTGCAGCTGCAGTAAGTTCA	*Pst*I, *Pvu*II
42	DP-L4104	70-RDIEELEK	GAAGTAAGTTCAGCTGCAATTGCGGCACTAGCAGCTTCGAATAAAGTG	*Pvu*II
43	DP-L4105	80-KVKNTNKAD	GAAAAATCGAATGCAGTGGCCAATACGAACGCAGCAGCTCTAATAGCA	*Hae*III
44	DP-L4106	94-KAKAEK	ATAGCAATGTTGGCGGCAGCTGCAGCGGCTGGTCCGAAT	*Pst*I, *Pvu*II
45	DP-L4107	109-EQTGNVAINEE	AATAACAACGGTGCGCAAACAGGAAATGTGGCTATAAATGCGGCCGCTTCAGGA	*Hae*III, *Not*I
46	DP-L4108	124-DRPTLQVERR	GCTTCAGGAGTCGCCGCACCAACTCTGCAAGTGGCGGCCGCTCATCCAGGT	*Hae*III, *Not*I
47	DP-L4109	140-DSAAEIKK	GGTCTGTCATCGGCTAGCGCAGCGGCAATTGCGGCCAGAAGAAAAGCC	*Hae*III
34	DP-L4110	146-KKRRK	GAAATTGCAGCAGCAGCAGCAGCCATAGCGTCGTCGGATAGT	Destroys *Mse*I
34			TATGGCTGCTGCTGCTGCTGCAATTTCCGCTGCGCTATCCGA	–
48	DP-L4111	156-DSELE	ATAGCGTCGTCGGCCAGTGCGCTTGCAAGCCTTACT	*Hae*III
49	DP-L4112	166-DKPTK	CTTACTTATCCAGCGGCCCCAACAGCAGCAAATAAG	*Hae*III
50	DP-L4113	173-KRKVAKE	ATAAACCAACAAAAGCAAATGCAGCTGCAGTGGCGGCGGCTTCAGTTGTGGATGCTTCTG	*Pst*I, *Pvu*II
50			CAGAAGCATCCACAACTGAAGCCGCCGCCACTGCAGCTGCATTTGCTTTTGTTGGTTTAT	–
51	DP-L4114	183-DASESDLD	GAGTCAGTTGTGGCCGCTTCTGCAAGTGCCTTAGCTTCTAGCATG	*Hae*III
52	DP-L4115	197-DE	ATGCAGTCAGCAGCGGCCTCTACACCACAACCTTTAGCAGCAAATCAA	*Hae*III
53	DP-L4116	209-KPFFPKVFKK	TTAAAAGCAAATCAAGCACCATTTTTCCCTGCAGTATTTGCGGCTATAAAAGATGCG	*Pst*I
54	DP-L4117	220-KDAGKWVRDK	GTATTTAAAAAAATAGCAGCTGCGGGGGCATGGGTAGCTGCTGCAATCGACGAA	*Pvu*II
55	DP-L4118	231-DENPEVKK	CGTGATAAAATCGCCGCAAATCCTGCAGTAGCAGCTGCGATTGTT	*Pvu*II
56	DP-L4119	242-DKSAGLID	AAAGCGATTGTTGCGGCCAGTGCAGGGTTAATTGCACAATTATTAACC	*Hae*III
57	DP-L4120	254-KKK	GACCAATTATTAACCGCGGCCGCAAGTGAAGAG	*Hae*III, *Not*I

a. Underlined amino acids were changed to alanine.
b. Underlined nucleotides indicate the newly introduced restriction enzyme site.

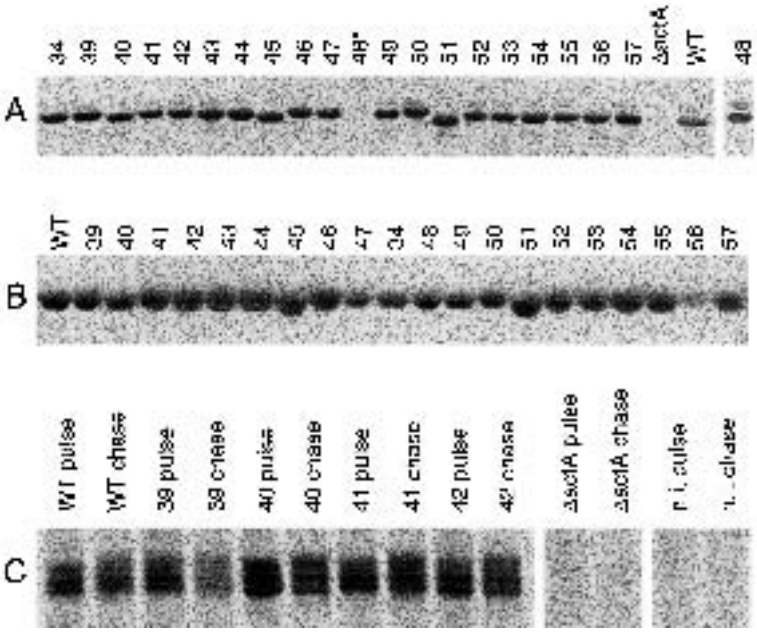

Fig. 2. A. Western blot detection of ActA expression from the mutant panel. Mutant numbers are noted above the lanes. Wild type and Δ*actA* controls are shown on right. Bacterial numbers were normalized by OD_{600}, and equivalent amounts were loaded in each lane. (*) Mutant 48 was reisolated after the first clone did not express ActA (right).
B. Coomassie blue protein gel of purified secreted ActA variants.
C. Pulse–chase labelling of a subset of ActA proteins in J774 host cells. A 30 min [^{35}S]-methionine pulse was followed by a 2 h chase. n.i., no infection control. Bacterial numbers were normalized by viable count, and equivalent numbers were loaded in each lane.

2.8 μm min^{-1} (± SD) (n = 8); mutant 39 rate: 15.4 ± 6.1 μm min^{-1} (± SD) (n = 10)). Mutant 34 (in the 'C' region) was not associated with actin and did not move in PtK2 cells. In MDCK cells, however, ≈ 75% of mutant 34 were associated with actin 4 h after infection and, in these cells, some of the bacteria moved at a slow rate (data not shown). It is not clear whether the ability to associate with actin and occasionally to induce motility in MDCK cells was a result of the intrinsic actin-binding properties of other regions of ActA or of the ability of this crippled protein to recruit and weakly activate the Arp2/3 complex.

Mutants had a range of phenotypes in intracellular spreading assays

We next tested the ability of each mutant to spread from cell to cell, an action that requires more factors than ActA, but is also completely dependent on ActA. One method of assessing cell-to-cell spread is to measure the plaque diameter resulting from *L. monocytogenes* infection in a monolayer of L2 cells (Sun *et al*., 1990). In this assay, an ActA null mutant does not form a plaque (Kocks *et al*., 1992; Skoble *et al*., 2000). The 20 mutants had a range of phenotypes in the plaque assay (Fig. 3D). Five had no discernible defect (mutants 45, 46, 47, 53 and 57). Eleven had small to intermediate reduction in plaque size of 65% to 90% of wild type. Two had severe plaque phenotypes (mutant 39 at 33%, mutant 48 at 41%), and two made no detectable plaque (mutants 34 and 56). It was surprising that mutant 56 made no plaque because a deletion of this region described previously (Δ202–263, strain DP-L3982) has a negligible effect on plaque size (Skoble *et al*., 2000). The 3-amino-acid change in mutant 56 caused a complete null plaquing phenotype and thus acted in a dominant manner to the deletion. We used allelic exchange to introduce the Δ202–263 allele into the mutant 56 strain to confirm that the null plaquing phenotype resulted from the specific *actA* mutation. In this strain (DP-L4121), referred to as 56 to Δ in Fig. 3D, plaque size was restored to nearly wild-type size, indicating that the reduction in plaquing efficiency of mutant 56 was caused by the specific *actA* mutation (Fig. 3D).

Eight mutations resulted in Arp2/3-mediated actin nucleation defects

ActA stimulates Arp2/3-dependent actin nucleation (Welch *et al*., 1998). Three regions in the NH_2-terminal domain of ActA have been shown to be critical for wild-type Arp2/3-dependent actin nucleation. The 'A' and 'C' regions interact directly with the Arp2/3 complex, and the 'AB' region is involved in actin monomer binding. Deletions in any of these regions have a decreased actin nucleation stimulating activity (Skoble *et al*., 2000). To define more precisely the residues involved in actin nucleation within the NH_2-terminal domain, we purified each ActA protein variant and tested them in the pyrene-actin polymerization assay. The pyrene-actin polymerization assay measures the increase in fluorescence over time when ActA, Arp2/3 complex and pyrene-labelled actin monomer are mixed. The data are represented quantitatively as 'fold stimulation' of actin polymerization stimulated by each protein variant over Arp2/3-dependent stimulation alone, which is defined as onefold stimulation. At an equimolar ratio of Arp2/3 to ActA, wild-type ActA stimulates Arp2/3-mediated actin nucleation 13.3-fold over Arp2/3 alone (Fig. 3E).

Only mutants that have had amino acid changes in the 'A', 'AB' and 'C' regions (mutants 39–48) had decreased activity in this assay, confirming what was reported previously (Skoble *et al.*, 2000). Four of the six mutants that overlapped the Arp2/3 interacting regions 'A' and 'C' had decreased nucleation-stimulating activities (Fig. 3E). The most critical residues for Arp2/3 stimulation were spanned by mutants 34 and 48 (both within the 'C' region). All the mutants that overlapped the actin-binding region ('AB', mutants 41–44) had intermediate defects in this assay. No Arp2/3-mediated actin nucleation defects were seen outside these previously defined regions, in either mutants that fell within the first 165 amino acids of the NH_2-terminus spanned by the 'A', 'AB' and 'C' regions, or mutants 49–57 that fell between amino acids 165 and 260. All the phenotypes associated with these mutants were therefore Arp2/3 and actin monomer binding independent.

Four changes resulted in actin monomer-binding defects

We next tested the ability of a subset of ActA variants to bind actin monomer in order to refine the 'AB' region. ActA binding to actin monomer *in vitro* inhibits spontaneous actin polymerization (Lasa *et al.*, 1997; Cicchetti *et al.*, 1999; Skoble *et al.*, 2000). Six of the ActA protein variants were assayed for the ability to alter actin polymerization: four in the 'AB' region and two that overlap a putative second actin binding site reported previously (Zalevsky *et al.*, 2001) as well as deletion variants spanning each respective region (Fig. 4). Mutants 41–44 all have decreased actin monomer-binding activity in this assay. Mutants 45, 46 and a deletion 'AB-2' (amino acids 102–135) inhibited actin polymerization the same as wild type, suggesting that amino acids spanned by these mutations do not play a role in actin binding.

Several mutations resulted in unusual intracellular motility phenotypes

Intracellular motility is a highly complex process that requires co-ordinated regulation of many host cytoskeletal factors. Comprehensive analysis of time-lapse videos revealed several unusual phenotypes associated with a subset of ActA NH_2-terminal mutations. All these phenotypes were incompletely penetrant, suggesting that there are more subtle interactions with various cytosolic

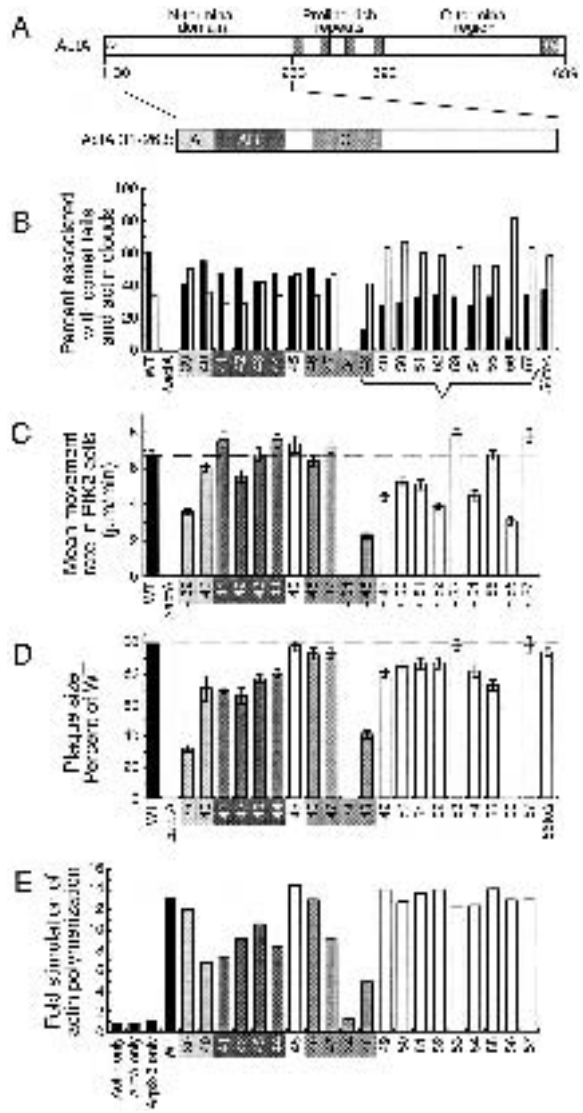

Fig. 3. Bar graph representation of quantitative data for ActA mutant panel.
A. Schematic representation of ActA with functional domains noted at the top. Amino acids 30–263 are enlarged with regions shown to be important for the function of ActA shown as shaded areas. 'A', acidic stretch; 'AB', actin-binding region; 'C', cofilin homology sequence. The NH_2-terminal domain is aligned with the bar graph representation of data (B–E) and shaded the same.
B. Percentage of bacteria associated with comet tails (black bars) and actin clouds (white bars) in PtK2 cells. Between 342–846 bacteria were scored in 10–15 PtK2 cells. A dashed line indicates wild-type level associated with comet tails; solid line indicates wild-type level associated with actin clouds. Mutants with an inverted ratio of actin clouds and comet tails are indicated by a bracket. Mutants are arranged in linear order from the most amino terminal to the most carboxy terminal and aligned schematically with the functional regions shown above. A strain containing a deletion of amino acids 202–263 is shown on the right.
C. Mean movement rate for each mutant strain in PtK2 cells. Error bars are standard error of the mean. Data represent 58–283 bacteria in 9–21 PtK2 cells. Bacterial strains are arranged as in (B). Statistically significant differences are denoted by an asterisk (*). A dashed line indicates the wild-type rate.
D. Plaque size made by each bacterial strain in an L2 monolayer. Wild type is defined as 100% (dashed line). A strain containing a deletion of amino acids 202–263 is shown on the right.
E. Fold stimulation of Arp2/3-mediated actin polymerization by purified ActA protein variants, as determined in the pyrene-actin polymerization assay. A dashed line indicates wild-type fold stimulation.

factors that are affected by these mutations. The unusual phenotypes are described in the following sections and are summarized in Table 2.

Mutant 42 made long protrusions at the edge of host cells

When a wild-type bacterium encounters the host cell membrane and proceeds into a pseudopod-like projection, there are several possible outcomes. It enters the protrusion and quickly returns to the same cell, proceeds into a neighbouring cell via cell-to-cell spread or extends about four to seven bacterial lengths from the host cell body and remains there for some time. In 60% of PtK2 cells observed, 5–15% of mutant 42 bacteria made extended protrusions and were observed up to 32.7 μm from the edge of the host cell (see *Supplementary material*). By comparison, the average length of wild-type protrusions was 8.4 μm, with a maximum measured length of 13.4 μm. However, most of the protrusions made by mutant 42 were indistinguishable from wild type. Long protrusions were not observed in any of the other mutants.

Mutant 50 had altered paths of intracellular motility compared with wild type

Wild-type bacteria generally move in gentle smooth arcing paths through the cytoplasm. In 42% of PtK2 cells observed, 30–50% of mutant 50 bacteria deviated from the wild-type motility path pattern, turning more frequently and in tighter circles than wild type (Fig. 5). Some bacteria appeared to spin around as if their front end was pinned in place. The actin tail of mutant 50 did not appear to be aberrant or mislocalized in fixed immunofluorescence images. Although it was not impossible to observe wild type moving in tight circles, it occurred at a much lower frequency (< 1% of bacteria).

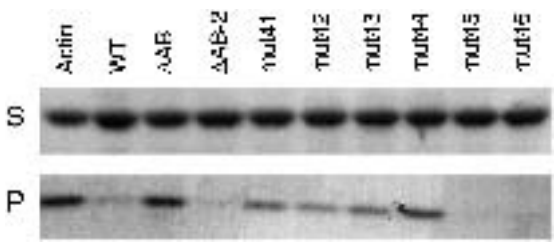

Fig. 4. Inhibition of actin polymerization by excess ActA. Actin pelleting in the presence of excess ActA was used to assess the ability of ActA variants to prevent actin polymerization. Actin filaments (F-actin) were separated from monomeric actin (G-actin) by centrifugation, and the amounts of F-actin in the pellet (P) and G-actin in the supernatant (S) were visualized on a 12% polyacrylamide gel stained with Coomassie blue. Protein variants are noted above. 'ΔAB' spans amino acids 60–101, 'ΔAB-2' spans amino acids 102–135.

Mutant 53 was associated with discontinuous actin tails in vivo

Actin tails associated with wild-type bacteria have a characteristic pattern of density that is most dense in the region closest to the bacterium and decreases gradually distal to the bacterium (Theriot *et al*., 1992). In 50% of infected PtK2 cells, 5–10% of mutant 53 had a 'discontinuous tail' phenotype (Fig. 6), in which the actin tails had alternating actin-rich and actin-sparse regions. This was a similar phenotype to that reported for an internal deletion in a different part of ActA (Δ50–126) (Lasa *et al*., 1997). Unlike the dramatic videos of bacteria stopping and starting in cell extracts from this previous study, a similar cyclic motility behaviour was not readily apparent in time-lapse videos of mutant 53. To our knowledge, this is the first report of discontinuous actin tails in host cells.

Mutant 55 'skidded' in the cytoplasm and had actin tails associated with the longitudinal surface

Mutant 55 often moved through the cytoplasm like wild type with one dramatic difference: it occasionally made very sharp turns, as if the bacterium was 'skidding', and had the actin tail extending from the side of the bacterium instead of the tail end (see *Supplementary material* and Fig. 7). In phase-contrast videos, 12% of bacteria skidded at least once in 5 min (138/1140 bacteria in 18 PtK2 cells), often when entering a protrusion. Wild type was only observed to skid four times in a comparable number of PtK2 cells (< 0.5%). In fixed immunofluorescence images, every cell observed had 2–5% of bacteria with actin tails extending from the lateral surface. We did not observe mislocalized tails for wild type or any other mutant. Skidding motility frequently occurred in localized regions within the host cell: in the immediate region in which one bacterium skidded, it was more likely that a second, third or fourth bacterium would exhibit the same motility behaviour. This often occurred near the periphery of the host cell. Additionally, in time-course videos, we observed that the tendency for wild-type bacteria to enter a protrusion was localized in a similar manner (data not shown), suggesting that skidding may be an abortive attempt to enter a protrusion.

Discussion

In this study, we constructed 20 new alleles of *actA* and used them to replace the chromosomal copy of *actA*. Eighteen of these were expressed at wild-type levels both *in vitro* and in host cells, validating the charged-to-alanine scanning mutagenesis approach. Using ActA purified from each of the mutants, we specifically defined the critical

Table 2. Unusual motility phenotypes *actA* mutants.

Mutant	Amino acids	Low penetrance phenotype
39	32–42	Slow movement rate in PtK2 cells, wild-type rate in MDCK cells
42	70–77	Long pseudopod-like protrusions
34	146–150	No movement in Ptk2 cells, moves slowly in MDCK cells
50	173–179	Altered paths through the cytoplasm of PtK2 cells
53	209–218	Discontinuous actin tails in PtK2 cells
55	231–238	Skidding, dramatic changes in direction, actin tails on bacterial side

residues involved in ActA's stimulation of the Arp2/3 complex, and more comprehensively characterized the actin-binding sequence. Further, we defined a previously unrecognized function for the NH_2-terminal domain in cloud-to-tail transition and intracellular motility rates.

Refining the 'A' and 'C' regions: critical residues for stimulation of the Arp2/3 complex

The acidic stretch ('A' region, amino acids 31–59) and the cofilin homology sequence ('C' region, amino acids 136–165) are involved in Arp2/3 activation as defined previously by deletion analysis (Skoble *et al*., 2000). Although there were severe *in vivo* phenotypes associated with mutant 39 ('A' region), the residues altered in this most NH_2-terminal mutant are not important for Arp2/3-dependent actin nucleation, but appear instead to have a role in the stability of the ActA protein in tissue culture cells. Although the tissue culture cell phenotypes associated with mutant 40 are less dramatic than those associated with mutant 39, purified protein from mutant 40 stimulates actin nucleation about half as well as wild type. Even though our data cannot preclude the involvement of hydrophobic residues contained within amino acids 31–59, they do narrow the charged residues of the 'A' region from amino acids 31–59 to amino acids 43–54 as being required for maximal Arp2/3-dependent actin nucleation.

The cofilin homology sequence spans 30 amino acids in the NH_2-terminus of ActA and contains nine amino acid identities plus five more conserved amino acids with human cofilin. The most important residues for activation of the Arp2/3 complex are amino acids 146–160, which reside in the cofilin homology sequence and are spanned by the contiguous mutants 34 and 48, both of which are severely impaired in all assays used in this study (Fig. 3B–E). Mutant 34, which changes 146-KKRRK-150, has the most severe set of phenotypes of the scan and has virtually no biochemical activity, whereas mutant 48 makes a small plaque, recruits actin to the bacterial surface less efficiently, moves more slowly and stimulates the Arp2/3 complex poorly. These data are in agreement with previous studies that have implicated this KKRRK sequence as being critical for the actin-based motility of *L. monocytogenes* (Lasa *et al*., 1997; Pistor *et al*., 2000; Skoble *et al*., 2000). Within this sequence, Pistor *et al*. (2000) evaluated the effect of these changes in PtK2 cells. The data suggest that 148-RR-149 played the most important role in actin polymerization *in vivo*, which is consistent with our results that mutant 47 (which includes 146-KK-147 but leaves 148-RR-149 unchanged) had less

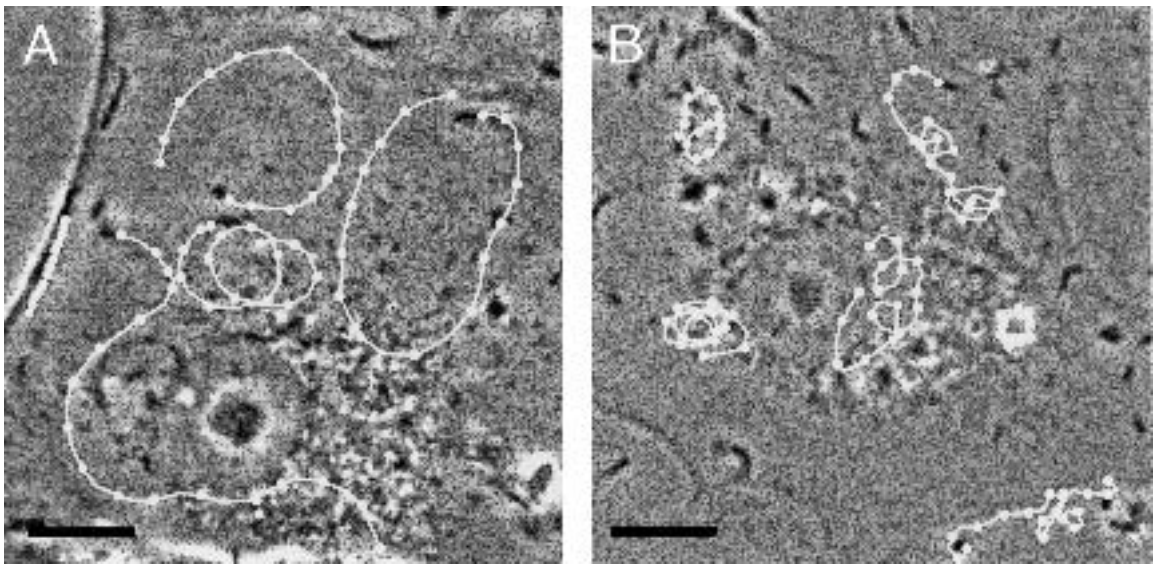

Fig. 5. Paths of (A) wild type and (B) mutant 50 over 5 min in PtK2 cells. Intervals (white dots) are 20 s. Scale bar is 10 μm.

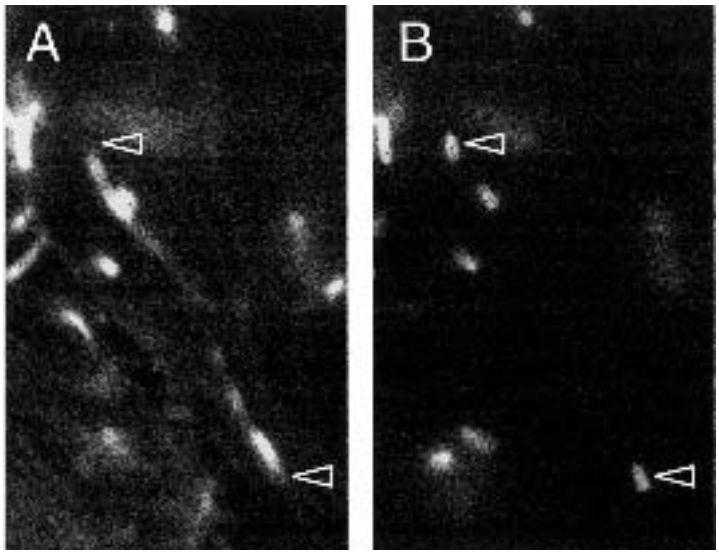

Fig. 6. Discontinuous actin tails associated with mutant 53 in PtK2 cells.
A. Actin and comet tails visualized with rhodamine–phalloidin.
B. The same as (A) except that bacteria are visualized with polyclonal anti-*Listeria* antibody. Bacteria associated with discontinuous actin tails are indicated by an open arrowhead.

severe defects in all assays we tested. As mutations 34 and 48 span a total of 15 amino acids, they may represent the core Arp2/3 activation domain for ActA.

The actin-binding domain spans 40 amino acids

The actin-binding domain ('AB' region, amino acids 60–101) is essential for the stimulation of actin polymerization, as measured by the Arp2/3 nucleation assay (Skoble *et al*., 2000). This region is dispensable *in vivo*, perhaps because of the ability to recruit actin binding proteins VASP and profilin via the central repeat region of ActA (Skoble *et al*., 2001). Mutants 41–44 span the actin-binding domain, and each of these 'AB' region mutants has similar phenotypes: statistically wild-type movement rates, form a plaque 70–80% of wild type and have a biochemical defect in the pyrene-actin nucleation assay. All four purified mutant proteins have an intermediate actin-binding activity. This strongly suggests that residues spanning the entire 40 amino acids of 'AB' are involved in actin monomer binding *in vitro*. Another possible biological role for the 'AB' region that is not excluded by these data is direct interaction with the actin-related proteins 2 and 3 of the Arp2/3 complex.

A recent report identified two actin binding sites in ActA (Zalevsky *et al*., 2001). The first site spanned amino acids 85–104 (overlapping the 'AB' region 60–101), the second actin binding site was more carboxy terminal in the ActA protein and spanned amino acids 121–138. The 'new' site ('AB-2') overlapped mutants 45 and 46. Mutants 45 and 46 had only slight, if any, phenotypes in all the biological assays. Furthermore, purified ActA from these two

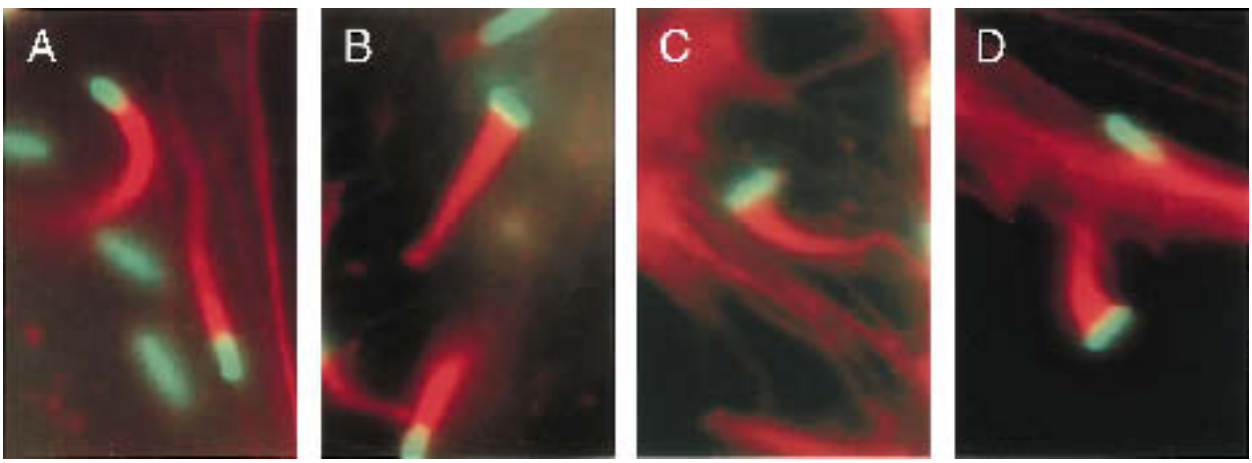

Fig. 7. Actin tails associated with the side of mutant 55 in PtK2 cells.
A. Actin tail localization of wild type.
B–D. Actin tail localization of mutant 55. Bacteria (green) were visualized with a polyclonal anti-*Listeria* antibody. Actin (red) was visualized with rhodamine–phalloidin.

mutants did not have biochemical defects in the Arp2/3 nucleation assay (Fig. 3E) or in the inhibition of actin polymerization assays (Fig. 4). The data presented here do not preclude the presence of two actin binding sites, but do not support localization for a second actin binding site between amino acids 121–138.

MUTT, a region involved in motility rates, unusual phenotypes and the actin cloud-to-tail transition spans amino acids 165–260, and these phenotypes suggest previously unrecognized functions for ActA in bacterial actin-based motility

A newly recognized region in the NH_2-terminus of ActA, amino acids 165–260, was involved in cloud-to-tail transition and intracellular motility rates. Mutants 49–57 were associated with more actin clouds than comet tails in cells, which was an inverse ratio from wild type (Fig. 3B). In addition, the same region had the largest cluster of mutants whose motility rates differed from wild type (Fig. 3C). Six of these mutants moved at slower motility rates (49–52, 54 and 56), and two moved at a faster rates (mutants 53 and 57). Only mutant 55 had a wild-type rate, but this mutant had an unusual skidding phenotype. These data suggest that this region was involved in the transition from actin nucleation at the bacterial surface to intracellular motility or the maintenance of motility once it was established.

We envision at least three possibilities for the phenotypes associated with mutants 49–57. This region may be important for: (i) association with host factors not currently known to play a role in *L. monocytogenes* actin-based motility; (ii) an indirect interaction with a known factor involved in actin-based motility; or (iii) proper localization of ActA on the bacterial surface.

ActA can interact biochemically with several phosphoinositides (Cicchetti *et al*., 1999; Steffen *et al*., 2000), although a biological role for this observation has yet to be established. PIP_2 directly stimulates the ability of Wiskott–Aldrich syndrome protein (WASP) to activate the Arp2/3 complex (Miki *et al*., 1996; Rohatgi *et al*., 1999), and WASP is thought to play the analogous role in eukaryotic cell motility that ActA plays in the movement of *L. monocytogenes* (Machesky *et al*., 1999). ActA variants deleted for the PIP_2 interacting region stimulate Arp2/3-dependent actin nucleation at wild-type levels *in vitro* (Skoble *et al*., 2000), suggesting that PIP_2 does not stimulate ActA directly. If ActA does bind PIP_2 *in vivo*, it therefore must have some role other than direct stimulation of the Arp2/3 complex. One possibility could be to regulate capping protein negatively, which prevents further elongation from the barbed ends of actin filaments. This capping function is inhibited by binding PIP_2 (Cooper and Schafer, 2000). ActA may increase the local concentration of PIP_2 near the bacterial surface and thus inhibit the activity of capping protein, effectively increasing the local concentration of barbed ends that are needed for the actin-based motility of *L. monocytogenes*. It has been suggested from thermodynamic studies of bacterial actin-based motility that *L. monocytogenes* maintains a local concentration of uncapped ends at the bacterial surface to allow the addition of actin monomer (Marchand *et al*., 1995). Alternatively to PIP_2, LaXp180, a mammalian protein of unknown function, has recently been demonstrated to interact with ActA and to co-localize with the front end of some intracellular bacteria (Pfeuffer *et al*., 2000). It is possible that this occasional co-localization may help to explain the unusual low penetrance phenotypes described in this study.

The second possible role for the MUTT region is interaction, possibly indirectly through a structural change in the ActA protein, with any of the factors already known to be involved in actin-based motility. These include actin monomer, the Arp2/3 complex and VASP. The motility rate phenotypes and lower percentage of actin tail-associated intracellular bacteria suggest that VASP would be the most likely candidate for this interaction, as VASP is directly involved in the rate bacteria move as well as in the percentage of moving bacteria in cells (Smith *et al*., 1996).

Another possible role for the MUTT region is the asymmetric localization of ActA on the surface of the bacterium. There are conflicting reports as to the relevance of asymmetry for the biological role of ActA. Purified ActA that is asymmetrically attached to either an unrelated bacterium or polystyrene beads is sufficient for actin-based motility in cell extracts, although polystyrene beads smaller than a bacterium do not require ActA asymmetry to initiate motility (Smith *et al*., 1995; Cameron *et al*., 1999). ActA has been reported to be both asymmetric on the surface of the bacterium (Kocks *et al*., 1993) and uniformly distributed on the bacterial surface (Niebuhr *et al*., 1993). If ActA does indeed have an asymmetric distribution on the bacterial surface, there must be a molecular mechanism to establish and/or maintain the asymmetry. The MUTT region may direct this localization through interaction with bacterial factors involved in establishing asymmetry. Consequently, the skidding phenotype of mutant 55 may be explained if the mutation causes the mislocalization of ActA more to the sides of the bacterium, leading to more actin associated with the longitudinal bacterial surfaces instead of the bacterial pole.

Several mutants have cell-dependent motility phenotypes

The phenotypes associated with several mutants suggest that caution is necessary when drawing general conclusions from data generated in a single cell type. For example, mutants at the NH_2-terminus of ActA and in the cofilin homology sequence had cell type-dependent

phenotypes. Mutant 34 appeared to be completely null in PtK2 cells, but nucleated actin and supported some bacterial movement in MDCK cells. Additionally, ActA containing a deletion of these five amino acids (146-KKRRK-150) expressed from a plasmid nucleates actin in *Xenopus laevis* cell extracts (Lasa *et al*., 1997). This, as well as the data that mutant 39 moved half as fast as wild type in PtK2 cells but at wild-type rates in MDCK cells, suggests that there are fundamental differences in the actin cytoskeletal dynamics between these two cell types. These differences may include the abundance of factors involved in actin dynamics (Arp2/3 complex, actin, VASP, capping protein, etc.) in these different circumstances. Although the variability in phenotypes complicates the functional dissection of ActA function, understanding the specific biochemical basis for these differences will provide key insights into the mechanism of ActA function.

Mechanical phenotypes will contribute to a full understanding of the mechanism of actin-based motility

The intracellular movement of *L. monocytogenes* has proved to be an extraordinarily useful model system for the molecular dissection of actin-based motility. Over the past decade, several laboratories have used a combination of *in vitro* biochemical assays and site-directed mutagenesis to identify the host cell components necessary for motility and to delineate their most important sites of association with ActA (Pistor *et al*., 1994; Friederich *et al*., 1995; Lasa *et al*., 1995; 1997; Smith *et al*., 1995; 1996; Skoble *et al*., 2000). The recent reconstitution of motility *in vitro* using only purified host cell proteins was a dramatic illustration of the success of this biochemical approach (Loisel *et al*., 1999). Now that the components sufficient for motility have been identified, the important questions in this field involve understanding how these specific proteins work together, co-ordinating their activities in space and in time, to organize the large-scale comet tail structure and to generate force and movement. Approaching these questions will require that we connect particular mechanical aspects of the system with its better understood biochemical aspects. Several of the novel mutant phenotypes we have uncovered in this systematic screen, particularly those affecting the cloud-to-tail transition, path curvature and persistence of motion or skidding, may represent useful handles for coupling biophysics with biochemistry. A detailed biochemical analysis of how these variant versions of ActA are altered in their specific interactions with each of the other protein components involved in motility will allow us to couple large-scale mechanical defects with individual small-scale protein–protein interactions. We expect that such physico-chemical analysis will contribute to a better integrated understanding of actin-based motility at all levels.

Experimental procedures

Bacterial strains, plasmids and DNA manipulations

The bacterial strains used in this study are described in Table 3. *L. monocytogenes* strains were propagated on brain–heart infusion (BHI) media with the appropriate antibiotic, when necessary. *Escherichia coli* strain XL1 Blue (Stratagene) was used for plasmid cloning, and strains were grown in LB media supplemented with the appropriate antibiotic. Restriction enzyme digests, ligations and DNA manipulations were performed using standard methods (Sambrook *et al*., 1989).

Construction of actA *mutant panel, secreted ActA variants and protein purification*

The *actA* DNA sequence encoding N-terminal amino acids 30–263 was divided arbitrarily into 20 sequence blocks that were amenable to M13 oligonucleotide-directed mutagenesis using established methods (Kunkel *et al*., 1991). Oligonucleotides were designed according to Wertman *et al*. (1992) (Table 1). Each mutation introduced a new 'silent' restriction site or removed an existing restriction site near the location of the mutagenesis. Eighteen of the *actA* alleles were constructed by this method. Mutant 34 was made using splicing by overlap extension polymerase chain reaction (SOE-PCR) (Horton *et al*., 1990). Mutant 50 was made using a Quikchange site-directed mutagenesis kit (Stratagene) on pDP-3934.

The allelic exchange vector pDP-3934 contains a 3.1 kb *Bam*H1–*Sac*II fragment from the 10403S chromosome cloned into the temperature-sensitive vector pKSV7 (Smith and Youngman, 1992). pDP-3934 contains >1 kb of DNA on either side of every mutation introduced into *actA*. Allelic exchange was used to place the mutation on the chromosome under the control of the endogenous promoter in single copy as described previously (Camilli *et al*., 1993).

Each mutant strain candidate was screened by PCR and restriction digestion for the appropriate change in restriction enzyme pattern (Table 1). Correct clones were sequenced to confirm the allele. Sequencing was performed on 909 bp PCR products amplified with primers 5′-TGTATTAGCGTATC ACGAGGAGGG-3′ and 5′-GATGGAGTAGGAGCATTAAAA CCG-3′.

Each allele was subcloned into pDP-2717 (Welch *et al*., 1998) for *in vitro* expression and purification of the mutant proteins as described previously (Skoble *et al*., 2000).

ActA expression in vitro *and* in vivo *pulse–chase determination of protein stability*

ActA expression in broth culture was determined as described previously (Skoble *et al*., 2000). Expression and stability of mutant ActA proteins was measured in the cytoplasm of J774 macrophage-like cells as described previously (Moors *et al*., 1999a).

Plaque assay

Plaquing was conducted in L2 cell monolayers as described previously (Sun *et al*., 1990). Digital images were imported

into CANVAS (Debena Software), and plaque diameters (20–30 per experiment) were measured and compared with 10403S. Eight to 10 independent experiments were conducted for each mutant strain.

Microscopic analysis of L. monocytogenes*-infected tissue culture cells*

Potoroo tridactylis kidney epithelia (PtK2) and green fluorescent protein (GFP) actin-expressing MDCK cells (Robbins *et al.*, 1999) were cultured in DMEM media supplemented with 10% fetal bovine serum (FBS). Subconfluent tissue culture cell monolayers were infected as described previously (Smith *et al.*, 1996). Four hours after infection, 5 min time-course phase-contrast videos were taken with frames captured at 10 s intervals using METAMORPH software (Universal Imaging). Individual bacteria were tracked in METAMORPH using the 'track points' function for the duration of the video. Data were exported to EXCEL (Microsoft) for data analysis. 'Rolling' 1 min averages were calculated, and the fastest 1 min window was used for statistical calculations. The

Table 3. Bacterial strains and plasmids.

Strain	Relevant genotype	Source or reference
E. coli		
CJ236	*dut1 ung1 thi1 relA1* (pCJ105 (Cm^r))	Kunkel *et al.* (1987)
XL1 Blue	*E. coli* cloning strain	Stratagene
L. monocytogenes		
10403S	Wild type	Bishop and Hinrichs (1987)
DP-L4101	Chromosomal *actA* mutant 39	This study
DP-L4102	Chromosomal *actA* mutant 40	This study
DP-L4103	Chromosomal *actA* mutant 41	This study
DP-L4104	Chromosomal *actA* mutant 42	This study
DP-L4105	Chromosomal *actA* mutant 43	This study
DP-L4106	Chromosomal *actA* mutant 44	This study
DP-L4107	Chromosomal *actA* mutant 45	This study
DP-L4108	Chromosomal *actA* mutant 46	This study
DP-L4109	Chromosomal *actA* mutant 47	This study
DP-L4110	Chromosomal *actA* mutant 34	This study
DP-L4111	Chromosomal *actA* mutant 48	This study
DP-L4112	Chromosomal *actA* mutant 49	This study
DP-L4113	Chromosomal *actA* mutant 50	This study
DP-L4114	Chromosomal *actA* mutant 51	This study
DP-L4115	Chromosomal *actA* mutant 52	This study
DP-L4116	Chromosomal *actA* mutant 53	This study
DP-L4117	Chromosomal *actA* mutant 54	This study
DP-L4118	Chromosomal *actA* mutant 55	This study
DP-L4119	Chromosomal *actA* mutant 56	This study
DP-L4120	Chromosomal *actA* mutant 57	This study
DP-L4121	Chromosomal *actA* mutant Δ202–263	This study
L. monocytogenes strains used for ActA purification		
DP-L3935	SLCC-5764 (ΔactA, Δmpl)	Skoble *et al.* (2000)
DP-L4010	DP-L3935 (pDP-2717; wild-type *actA* allele)	Skoble *et al.* (2000)
DP-L4201	DP-L3935 (pDP-2717; mutant 39 *actA* allele)	This study
DP-L4202	DP-L3935 (pDP-2717; mutant 40 *actA* allele)	This study
DP-L4203	DP-L3935 (pDP-2717; mutant 41 *actA* allele)	This study
DP-L4204	DP-L3935 (pDP-2717; mutant 42 *actA* allele)	This study
DP-L4205	DP-L3935 (pDP-2717; mutant 43 *actA* allele)	This study
DP-L4206	DP-L3935 (pDP-2717; mutant 44 *actA* allele)	This study
DP-L4207	DP-L3935 (pDP-2717; mutant 45 *actA* allele)	This study
DP-L4208	DP-L3935 (pDP-2717; mutant 46 *actA* allele)	This study
DP-L4209	DP-L3935 (pDP-2717; mutant 47 *actA* allele)	This study
DP-L4210	DP-L3935 (pDP-2717; mutant 34 *actA* allele)	This study
DP-L4211	DP-L3935 (pDP-2717; mutant 48 *actA* allele)	This study
DP-L4212	DP-L3935 (pDP-2717; mutant 49 *actA* allele)	This study
DP-L4213	DP-L3935 (pDP-2717; mutant 50 *actA* allele)	This study
DP-L4214	DP-L3935 (pDP-2717; mutant 51 *actA* allele)	This study
DP-L4215	DP-L3935 (pDP-2717; mutant 52 *actA* allele)	This study
DP-L4216	DP-L3935 (pDP-2717; mutant 53 *actA* allele)	This study
DP-L4217	DP-L3935 (pDP-2717; mutant 54 *actA* allele)	This study
DP-L4218	DP-L3935 (pDP-2717; mutant 55 *actA* allele)	This study
DP-L4219	DP-L3935 (pDP-2717; mutant 56 *actA* allele)	This study
DP-L4220	DP-L3935 (pDP-2717; mutant 57 *actA* allele)	This study
DP-L3978	DP-L3935 (pDP-2717; Δ60–101 (ΔAB) *actA* allele)	Skoble *et al.* (2000)
DP-L4226	DP-L3935 (pDP-2717; Δ102–135 (ΔAB-2) *actA* allele	This study

rank sum test was used to determine statistically significant differences from wild-type movement rates.

Quantification of the percentage of bacteria associated with actin clouds and comet tails was done in PtK2 cells as described previously (Skoble *et al*., 2000).

Arp2/3-mediated pyrene-actin curves

Pyrene-actin curves were performed as described previously (Skoble *et al*., 2000). Purified His-tagged ActA was used at a concentration of 20 nM. Human Arp2/3 complex purified from platelets (Welch and Mitchison, 1998) was used at a concentration of 20 nM. For the calculation of fold stimulation, the maximal slope for each pyrene curve was determined and divided by the maximal slope of Arp2/3-only mediated stimulation of actin polymerization.

Inhibition of actin polymerization assay

Actin-binding assays were conducted as described previously (Skoble *et al*., 2000).

Acknowledgements

We would like to thank Victoria Auerbuch, Jennifer Robbins and Susanne Rafelski for stimulating discussions during the course of this work as well as methods and reagents. We are grateful to Nick Burrows-Brown and Lawrence Haines for technical assistance. We also thank Katerina Kechris for statistical advice in the analysis of movement rates, and Hélène Maquis for comments on the manuscript. This work was supported by US Public Health Service grants AI29619 (D.A.P.), GM59609 (M.D.W.), AI36929 and a Fellowship in Science and Engineering from the David and Lucile Packard Foundation (J.A.T.).

Supplementary material

The following material is available from http://www.blackwell-science.com/products/journals/suppmat/mole/mole2677/mmi2677sm.htm

Video supplement 1

Long protrusion phenotype of mutant 42. PtK2 cell is at the top of the field, and the bacteria are in extended protrusions extending down from the cell. Total time elapsed is 5 min.

Video supplements 2 and 3

Skidding phenotype of mutant 55. Two examples of skidding with associated relocalization of the actin tail, particularly visible in supplement 2 during the two sharp right-hand turns, where the actin tail temporarily relocates to the side of the bacterium.

Videos are the same time sequence repeated twice, the second time at half the speed of the first time. Tracks of the bacterial movement are overlaid (red) with each dot representing a 10 s interval.

References

Bass, S.H., Mulkerrin, M.G., and Wells, J.A. (1991) A systematic mutational analysis of hormone-binding determinants in the human growth hormone receptor. *Proc Natl Acad Sci USA* **88**: 4498–4502.

Bishop, D.K., and Hinrichs, D.J. (1987) Adoptive transfer of immunity to *Listeria monocytogenes*. The influence of *in vitro* stimulation on lymphocyte subset requirements. *J Immunol* **139**: 2005–2009.

Brundage, R.A., Smith, G.A., Camilli, A., Theriot, J.A., and Portnoy, D.A. (1993) Expression and phosphorylation of the *Listeria monocytogenes* ActA protein in mammalian cells. *Proc Natl Acad Sci USA* **90**: 11890–11894.

Cameron, L.A., Footer, M.J., van Oudenaarden, A., and Theriot, J.A. (1999) Motility of ActA protein-coated microspheres driven by actin polymerization. *Proc Natl Acad Sci USA* **96**: 4908–4913.

Camilli, A., Tilney, L.G., and Portnoy, D.A. (1993) Dual roles of *plcA* in *Listeria monocytogenes* pathogenesis. *Mol Microbiol* **8**: 143–157.

Chakraborty, T., Ebel, F., Domann, E., Niebuhr, K., Gerstel, B., Pistor, S., *et al.* (1995) A focal adhesion factor directly linking intracellularly motile *Listeria monocytogenes* and *Listeria ivanovii* to the actin-based cytoskeleton of mammalian cells. *EMBO J* **14**: 1314–1321.

Cicchetti, G., Maurer, P., Wagener, P., and Kocks, C. (1999) Actin and phosphoinositide binding by the ActA protein of the bacterial pathogen *Listeria monocytogenes*. *J Biol Chem* **274**: 33616–33626.

Cooper, J.A., and Schafer, D.A. (2000) Control of actin assembly and disassembly at filament ends. *Curr Opin Cell Biol* **12**: 97–103.

Cossart, P., and Lecuit, M. (1998) Interactions of *Listeria monocytogenes* with mammalian cells during entry and actin-based movement: bacterial factors, cellular ligands and signaling. *EMBO J* **17**: 3797–3806.

Dabiri, G.A., Sanger, J.M., Portnoy, D.A., and Southwick, F.S. (1990) *Listeria monocytogenes* moves rapidly through the host-cell cytoplasm by inducing directional actin assembly. *Proc Natl Acad Sci USA* **87**: 6068–6072.

Domann, E., Wehland, J., Rohde, M., Pistor, S., Hartl, M., Goebel, W., *et al.* (1992) A novel bacterial virulence gene in *Listeria monocytogenes* required for host cell microfilament interaction with homology to the proline-rich region of vinculin. *EMBO J* **11**: 1981–1990.

Farber, J.M., and Peterkin, P.I. (1991) *Listeria monocytogenes*, a food-borne pathogen. *Microbiol Rev* **55**: 476–511.

Friederich, E., Gouin, E., Hellio, R., Kocks, C., Cossart, P., and Louvard, D. (1995) Targeting of *Listeria monocytogenes* ActA protein to the plasma membrane as a tool to dissect both actin-based cell morphogenesis and ActA function. *EMBO J* **14**: 2731–2744.

Gibbs, C.S., and Zoller, M.J. (1991) Rational scanning mutagenesis of a protein kinase identifies functional regions involved in catalysis and substrate interactions. *J Biol Chem* **266**: 8923–8931.

Horton, R.M., Cai, Z.L., Ho, S.N., and Pease, L.R. (1990) Gene splicing by overlap extension: tailor-made genes using the polymerase chain reaction. *Biotechniques* **8**: 528–535.

Kocks, C., Gouin, E., Tabouret, M., Berche, P., Ohayon, H., and Cossart, P. (1992) *L. monocytogenes*-induced actin assembly requires the *actA* gene product, a surface protein. *Cell* **68**: 521–531.

Kocks, C., Hellio, R., Gounon, P., Ohayon, H., and Cossart, P. (1993) Polarized distribution of *Listeria monocytogenes* surface protein ActA at the site of directional actin assembly. *J Cell Sci* **105**: 699–710.

Kocks, C., Marchand, J.B., Gouin, E., d'Hauteville, H., Sansonetti, P.J., Carlier, M.F., and Cossart, P. (1995) The unrelated surface proteins ActA of *Listeria monocytogenes* and IcsA of *Shigella flexneri* are sufficient to confer actin-based motility on *Listeria innocua* and *Escherichia coli* respectively. *Mol Microbiol* **18**: 413–423.

Kunkel, T.A., Roberts, J.D., and Zakour, R.A. (1987) Rapid and efficient site-specific mutagenesis without phenotypic selection. *Methods Enzymol* **154**: 367–382.

Kunkel, T.A., Bebenek, K., and McClary, J. (1991) Efficient site-directed mutagenesis using uracil-containing DNA. *Methods Enzymol* **204**: 125–139.

Lasa, I., David, V., Gouin, E., Marchand, J.B., and Cossart, P. (1995) The amino-terminal part of ActA is critical for the actin-based motility of *Listeria monocytogenes*; the central proline-rich region acts as a stimulator. *Mol Microbiol* **18**: 425–436.

Lasa, I., Gouin, E., Goethals, M., Vancompernolle, K., David, V., Vandekerckhove, J., and Cossart, P. (1997) Identification of two regions in the N-terminal domain of ActA involved in the actin comet tail formation by *Listeria monocytogenes*. *EMBO J* **16**: 1531–1540.

Loisel, T.P., Boujemaa, R., Pantaloni, D., and Carlier, M.F. (1999) Reconstitution of actin-based motility of *Listeria* and *Shigella* using pure proteins. *Nature* **401**: 613–616.

Machesky, L.M., and Gould, K.L. (1999) The Arp2/3 complex: a multifunctional actin organizer. *Curr Opin Cell Biol* **11**: 117–121.

Machesky, L.M., Mullins, R.D., Higgs, H.N., Kaiser, D.A., Blanchoin, L., May, R.C., *et al.* (1999) Scar, a WASp-related protein, activates nucleation of actin filaments by the Arp2/3 complex. *Proc Natl Acad Sci USA* **96**: 3739–3744.

Marchand, J.B., Moreau, P., Paoletti, A., Cossart, P., Carlier, M.F., and Pantaloni, D. (1995) Actin-based movement of *Listeria monocytogenes*: actin assembly results from the local maintenance of uncapped filament barbed ends at the bacterium surface. *J Cell Biol* **130**: 331–343.

May, R.C., Hall, M.E., Higgs, H.N., Pollard, T.D., Chakraborty, T., Wehland, J., *et al.* (1999) The Arp2/3 complex is essential for the actin-based motility of *Listeria monocytogenes*. *Curr Biol* **9**: 759–762.

Miki, H., Miura, K., and Takenawa, T. (1996) N-WASP, a novel actin-depolymerizing protein, regulates the cortical cytoskeletal rearrangement in a PIP_2-dependent manner downstream of tyrosine kinases. *EMBO J* **15**: 5326–5335.

Moors, M.A., Auerbuch, V., and Portnoy, D.A. (1999a) Stability of the *Listeria monocytogenes* ActA protein in mammalian cells is regulated by the N-end rule pathway. *Cell Microbiol* **1**: 249–257.

Moors, M.A., Levitt, B., Youngman, P., and Portnoy, D.A. (1999b) Expression of listeriolysin O and ActA by intracellular and extracellular *Listeria monocytogenes*. *Infect Immun* **67**: 131–139.

Mounier, J., Ryter, A., Coquis-Rondon, M., and Sansonetti, P.J. (1990) Intracellular and cell-to-cell spread of *Listeria monocytogenes* involves interaction with F-actin in the enterocytelike cell line Caco-2. *Infect Immun* **58**: 1048–1058.

Mourrain, P., Lasa, I., Gautreau, A., Gouin, E., Pugsley, A., and Cossart, P. (1997) ActA is a dimer. *Proc Natl Acad Sci USA* **94**: 10034–10039.

Niebuhr, K., Chakraborty, T., Rohde, M., Gazlig, T., Jansen, B., Kollner, P., and Wehland, J. (1993) Localization of the ActA polypeptide of *Listeria monocytogenes* in infected tissue culture cell lines: ActA is not associated with actin 'comets'. *Infect Immun* **61**: 2793–2802.

Pfeuffer, T., Goebel, W., Laubinger, J., Bachmann, M., and Kuhn, M. (2000) LaXp180, a mammalian ActA binding protein, identified with the yeast two-hybrid system, co-localizes with intracellular *Listeria monocytogenes*. *Cell Microbiol* **2**: 101–114.

Pistor, S., Chakraborty, T., Niebuhr, K., Domann, E., and Wehland, J. (1994) The ActA protein of *Listeria monocytogenes* acts as a nucleator inducing reorganization of the actin cytoskeleton. *EMBO J* **13**: 758–763.

Pistor, S., Grobe, L., Sechi, A.S., Domann, E., Gerstel, B., Machesky, L.M., *et al.* (2000) Mutations of arginine residues within the 146-KKRRK-150 motif of the ActA protein of *Listeria monocytogenes* abolish intracellular motility by interfering with the recruitment of the Arp2/3 complex. *J Cell Sci* **113**: 3277–3287.

Robbins, J.R., Barth, A.I., Marquis, H., de Hostos, E.L., Nelson, W.J., and Theriot, J.A. (1999) *Listeria monocytogenes* exploits normal host cell processes to spread from cell to cell. *J Cell Biol* **146**: 1333–1350.

Rohatgi, R., Ma, L., Miki, H., Lopez, M., Kirchhausen, T., Takenawa, T., and Kirschner, M.W. (1999) The interaction between N-WASP and the Arp2/3 complex links Cdc42-dependent signals to actin assembly. *Cell* **97**: 221–231.

Sambrook, J., Maniatis, T., and Fritsch, E.F. (1989) *Molecular Cloning: A Laboratory Manual*, 2nd edn. Cold Spring Harbor, NY: Cold Spring Harbor Laboratory Press.

Skoble, J., Portnoy, D.A., and Welch, M.D. (2000) Three regions within ActA promote Arp2/3 complex-mediated actin nucleation and *Listeria monocytogenes* motility. *J Cell Biol* **150**: 527–538.

Skoble, J., Auerbuch, V., Goley, E.D., Welch, M.D., and Portnoy, D.A. (2001) Pivotal role of VASP in Arp2/3 complex-mediated actin nucleation, actin branch-formation and *Listeria monocytogenes* motility. *J Cell Biol* **155**: 89–100.

Smith, G.A., Portnoy, D.A., and Theriot, J.A. (1995) Asymmetric distribution of the *Listeria monocytogenes* ActA protein is required and sufficient to direct actin-based motility. *Mol Microbiol* **17**: 945–951.

Smith, G.A., Theriot, J.A., and Portnoy, D.A. (1996) The tandem repeat domain in the *Listeria monocytogenes* ActA protein controls the rate of actin-based motility, the percentage of moving bacteria, and the localization of vasodilator-stimulated phosphoprotein and profilin. *J Cell Biol* **135**: 647–660.

Smith, K., and Youngman, P. (1992) Use of a new integrational vector to investigate compartment-specific

expression of the *Bacillus subtilis spoIIM* gene. *Biochimie* **74**: 705–711.

Steffen, P., Schafer, D.A., David, V., Gouin, E., Cooper, J.A., and Cossart, P. (2000) *Listeria monocytogenes* ActA protein interacts with phosphatidylinositol 4,5-bisphosphate *in vitro*. *Cell Motil Cytoskeleton* **45**: 58–66.

Sun, A.N., Camilli, A., and Portnoy, D.A. (1990) Isolation of *Listeria monocytogenes* small-plaque mutants defective for intracellular growth and cell-to-cell spread. *Infect Immun* **58**: 3770–3778.

Theriot, J.A., Mitchison, T.J., Tilney, L.G., and Portnoy, D.A. (1992) The rate of actin-based motility of intracellular *Listeria monocytogenes* equals the rate of actin polymerization. *Nature* **357**: 257–260.

Theriot, J.A., Rosenblatt, J., Portnoy, D.A., Goldschmidt-Clermont, P.J., and Mitchison, T.J. (1994) Involvement of profilin in the actin-based motility of *L. monocytogenes* in cells and in cell-free extracts. *Cell* **76**: 505–517.

Tilney, L.G., and Portnoy, D.A. (1989) Actin filaments and the growth, movement, and spread of the intracellular bacterial parasite, *Listeria monocytogenes*. *J Cell Biol* **109**: 1597–1608.

Welch, M.D., and Mitchison, T.J. (1998) Purification and assay of the platelet Arp2/3 complex. *Methods Enzymol* **298**: 52–61.

Welch, M.D., Rosenblatt, J., Skoble, J., Portnoy, D.A., and Mitchison, T.J. (1998) Interaction of human Arp2/3 complex and the *Listeria monocytogenes* ActA protein in actin filament nucleation. *Science* **281**: 105–108.

Wertman, K.F., Drubin, D.G., and Botstein, D. (1992) Systematic mutational analysis of the yeast *ACT1* gene. *Genetics* **132**: 337–350.

Yarar, D., To, W., Abo, A., and Welch, M.D. (1999) The Wiskott–Aldrich syndrome protein directs actin-based motility by stimulating actin nucleation with the Arp2/3 complex. *Curr Biol* **9**: 555–558.

Zalevsky, J., Grigorova, I., and Mullins, R.D. (2001) Activation of the Arp2/3 complex by the *Listeria* ActA protein. ActA binds two actin monomers and three subunits of the Arp2/3 complex. *J Biol Chem* **276**: 3468–3475.